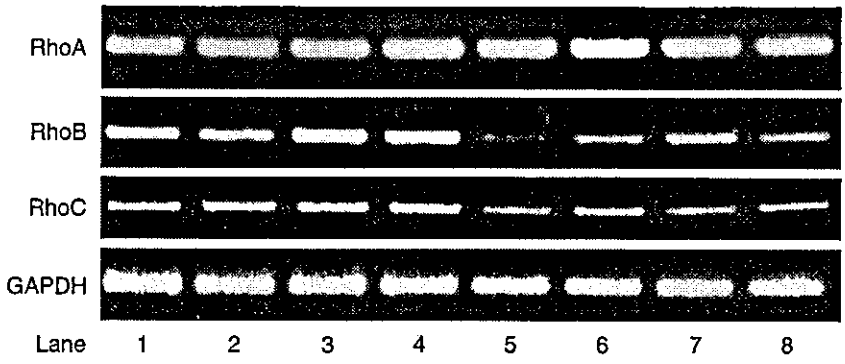

Fig. 1. mRNA expression in unilateral ureteral obstructed (UUO) mouse kidney 4 days after surgery. Results of RT-PCR of RNA from UUO mouse kidneys 4 days after surgery are shown. Each lane represents RT-PCR product from vehicle-treated obstructed kidneys (lanes 1 to 4) and contralateral kidneys (lanes 5 to 8).

method modified by Hansen, Nielsen and Berg [30]. Renal fibroblasts (p8, 4×10^3 cells/well) were introduced to 96-well plates. After 24 hours of serum starvation, DMEM containing 0.5% or 10% FCS and different concentrations of Y-27632 (0, 2, 20, 200 or 2000 μmol/L) was added. Twenty-four hours later, MTT (Sigma) was added to each well, and after a two hour incubation, extraction buffer [20% wt/vol of SDS dissolved in 50% N,N-dimethyl formaldehyde (DMF) solution, pH 4.7] was added. After overnight incubation, the optical densities at 595 nm were measured using an Emax precision microplate reader (Molecular Devices, Sunnyvale, CA, USA).

Cell migration assay

Migration of cultured macrophages was assayed using Cell Culture Insert with a pore size of 8.0 μm (Becton Dickinson, Franklin Lakes, NJ, USA). RAW 264.7 cells (2×10^5 cells) were introduced onto the insert. Cells were pre-incubated with DMEM containing 0.5% FCS or C3 exoenzyme (Biomol Research Laboratories Plymouth Meeting, PA, USA) for 24 hours. Serum-free DMEM containing either MCP-1 (2.5 ng/mL or 25 ng/mL; Sigma) or Ang II (1 μmol/L; Sigma) was added to the insert (0.4 mL) and the bottom chamber (1.4 mL) with Y-27632 (0, 10 or 100 μmol/L). After a 24-hour incubation, cells were fixed with methanol for 10 minutes and stained with Giemsa for 30 minutes at room temperature. The number of cells that remained on the inner surface of the insert and that had moved to its outer side through the pores was counted under a light microscope by changing the focus. Ten individual microscopic fields (×400) were selected at random in each section. Three individual experiments were performed. The scores of the ten fields of each section were averaged, and the scores of three separate experiments were then averaged. The proportion of migrated cells (Migration Index) was calculated as follows: Migration Index (%) = Cell number on outer side/Cell numbers on both sides × 100 [31].

Analytical procedure

All values are expressed as means ± standard deviation. The data were analyzed for homogeneity using Bartlett's test. The statistical significance of any intergroup differences was determined using Dunnett's test for homogeneous data or Kruskal-Wallis test followed by Dunnett's type test for heterogeneous data. Statistically significant differences between groups were defined as P values less than 0.05.

RESULTS

Drug delivery in UUO mice

Y-27632 was administered to mice orally by adding to the drinking water. During a series of experiment, there was no dropout due to death. In the preliminary experiment, water intake was significantly reduced in the Y-27632-treated group possibly due to the bitter taste of the drug. To overcome this problem, sucrose was added to the drinking water. Consequently, water intake of vehicle-treated mice became 4.50 ± 0.46 mL/day and that of Y-27632-treated animals became 4.42 ± 0.48 mL/day; the difference was not significant. Daily water intake in the Y-27632-treated group resulted in drug ingestion of about 40 mg/kg/day. The serum concentration of Y-27632 was 215.2 ± 82.3 ng/mL (0.64 μmol/L), which was similar to the reported Ki value of Y-27632 toward ROCKs in vitro.

Expression of Rho mRNA in UUO kidneys

Expression of RhoA, RhoB and RhoC mRNA four days after ureteral obstruction was examined by RT-PCR. While RhoA mRNA expression was not significantly different between UUO and contralateral kidneys, expression of RhoB and RhoC mRNA was up-regulated in UUO kidneys (Fig. 1).

Effects of Y-27632 on interstitial expansion of UUO kidneys

The representative appearance of Masson's trichrome-stained sections 10 days after ureteral obstruction is shown in Figure 2A. Interstitial expansion of obstructed kidneys was prominent in vehicle-treated animals (Fig. 2A, I). In Y-27632-treated animals, interstitial expansion

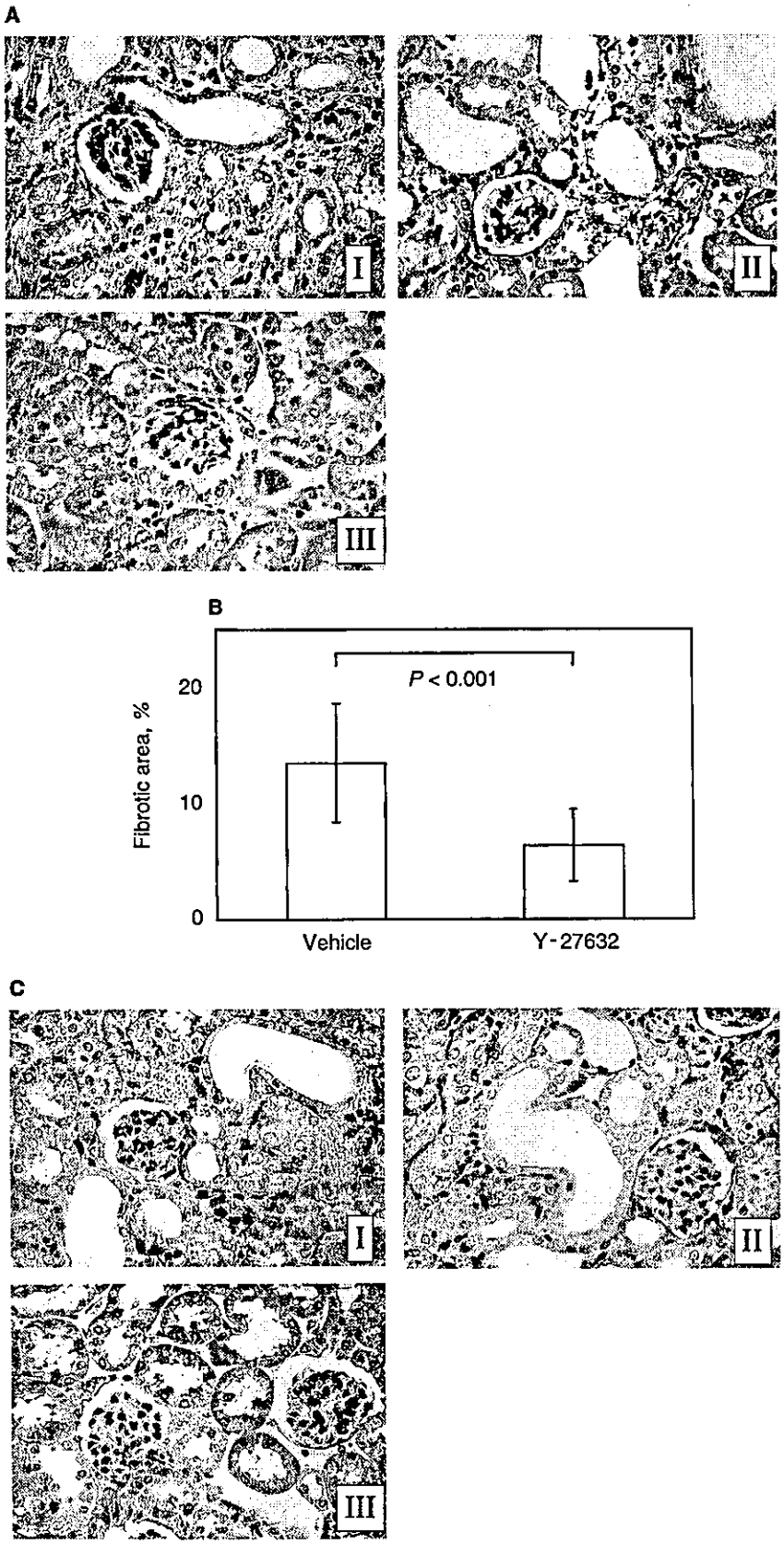

Fig. 2. Masson's trichrome staining of kidneys from both experimental groups at 4 and 10 days after ureteral obstruction and quantitative analysis of interstitial fibrosis. (*A*) Light-field photomicrographs of Masson's trichrome-stained sections of renal cortical region from (*I*) vehicle and (*II*) Y-27632-treated mouse obstructed kidneys 10 days after ureteral obstruction and (*III*) contralateral kidneys (×400). (*B*) Interstitial fibrosis was quantified with a computer-aided image manipulator. Five animals were analyzed for each group and 10 randomly selected high power fields were quantified and averaged to obtain the value for each animal. (*C*) Light-field photomicrographs of Masson's trichrome-stained sections of renal cortical region from (*I*) vehicle and (*II*) Y-27632-treated mouse obstructed kidneys 4 days after ureteral obstruction and (*III*) contralateral kidneys (×400).

was less than that in vehicle-treated controls and the tubular back-to-back structure was relatively well preserved (Fig. 2A, II). Y-27632 treatment significantly ameliorated the interstitial expansion in UUO kidneys at 10 days after ureteral obstruction to 47% of that in vehicle-treated controls (Fig. 2B). The effect of Y-27632 treatment on UUO kidneys after four days was not significant (Fig. 2C).

Effects of Y-27632 on interstitial SMαA expression in UUO kidneys

Induction of interstitial myofibroblasts was assessed by immunohistochemical detection of SMαA. Positive staining for SMαA was seen in vascular smooth muscle cells, but not in the interstitial space in the contralateral kidney (Fig. 3A, III). Intense immunostaining of SMαA was observed in periglomerular and peritubular interstitium in addition to the vascular smooth muscle cells of the arterioles in vehicle-treated mouse kidneys 10 days after ureteral ligation (Fig. 3A, I). Y-27632 treatment reduced the appearance of SMαA-positive myofibroblasts in the interstitium (Fig. 3A, II). The result of quantitative analysis of SMαA immunostaining are shown in Figure 3B). Y-27632 significantly reduced SMαA immunostaining at 10 days after ureteral obstruction to 50% of that in vehicle-treated controls.

Effects of Y-27632 on macrophage infiltration in the interstitium of UUO kidneys

Figure 4A shows the representative appearance of immunostaining for F4/80, a macrophage marker, in the UUO kidneys 10 days after ureteral obstruction in both experimental groups. At 10 days following ureteral obstruction, macrophage infiltration was observed in the periglomerular and peritubular interstitium of the obstructed kidneys from vehicle-treated mice (Fig. 4A, I). This was reduced in Y-27632-treated animals (Fig. 4A, II). Quantitative analysis of the F4/80-positive area in the interstitium is shown in Figure 4B. Significant reduction of the F4/80-positive area was observed in Y-27632 treated mouse kidneys to 51% of that in vehicle-treated controls.

Effects of Y-27632 on mRNA expression in obstructed kidneys and cultured renal fibroblasts

Expression of α1(I) collagen, SMαA and TGF-β mRNA 4 and 10 days after ureteral obstruction was examined to elucidate the effects of Y-27632 on fibrosis-related gene expression. Significant reductions were seen in α1(I) collagen, SMαA and TGF-β mRNA levels in the Y-27632-treated group (Fig. 5A and Table 2). Y-27632 treatment also reduced expression of SMαA mRNA in cultured renal fibroblasts in a dose-dependent manner (Fig. 5B), but reductions of α1(I) collagen and TGF-β mRNA levels in cultured renal fibroblasts were not significant (data not shown). Expression of osteopontin, MCP-1 and ICAM-1 mRNA 4 and 10 days after ureteral obstruction was examined to assess the production of chemokines, which are closely related to fibrosis in the UUO kidney. Only marginal suppression (less than 17%) of chemokine expression was observed in Y-27632-treated mice (Fig. 5A and Table 2).

Effects of Y-27632 on mouse renal fibroblast proliferation

We examined whether Y-27632 suppresses cell proliferation. MTT assay indicated that Y-27632 did not show an inhibitory effect on proliferation of mouse renal fibroblasts even at a dose of 200 μmol/L, and showed cytotoxicity at a dose of 2,000 μmol/L (Fig. 6).

Effects of Y-27632 on macrophage migration

While histological assessment showed that macrophage infiltration was significantly reduced in the Y-27632–treated group, Northern blot analyses showed that Y-27632 did not suppress typical macrophage chemokine mRNA expression. Therefore, we examined whether Y-27632 directly suppressed macrophage motility.

Y-27632 abrogated MCP-1–induced macrophage migration in a dose-dependent manner, indicating the involvement of Rho in cell motility. This is supported by the fact that C3 exoenzyme, inhibitor of Rho, also abrogated MCP-1–mediated migration of macrophage (Fig. 7A). We also examined whether Ang II stimulates chemotaxis. As shown in Figure 7B, Ang II stimulated macrophage migration and it was significantly suppressed by Y-27632.

DISCUSSION

The possible involvement of Rho signal transduction in the pathogenesis of progressive tissue damage including kidney disease has not been well investigated. This is the first trial to examine the pathophysiological significance of Rho in kidney disease. We hypothesized that Rho signal transduction is related to cell migration and proliferation in the lesions of progressive fibrosis. The present study was performed to elucidate whether Rho signal transduction is involved in the process of renal fibrosis, and if so, to assess the therapeutic value of Y-27632, a specific ROCK inhibitor.

We focused on tubulointerstitial lesions employing UUO model mice because tubulointerstitial injury invariably is found in the chronically diseased kidney, irrespective of the type of disease or the compartment in which the disease originated, and recent investigations revealed close association between interstitial damage and the prognosis of renal dysfunction [32, 33].

The expression of RhoB and RhoC mRNA was upregulated in UUO kidneys. Although pathophysiological

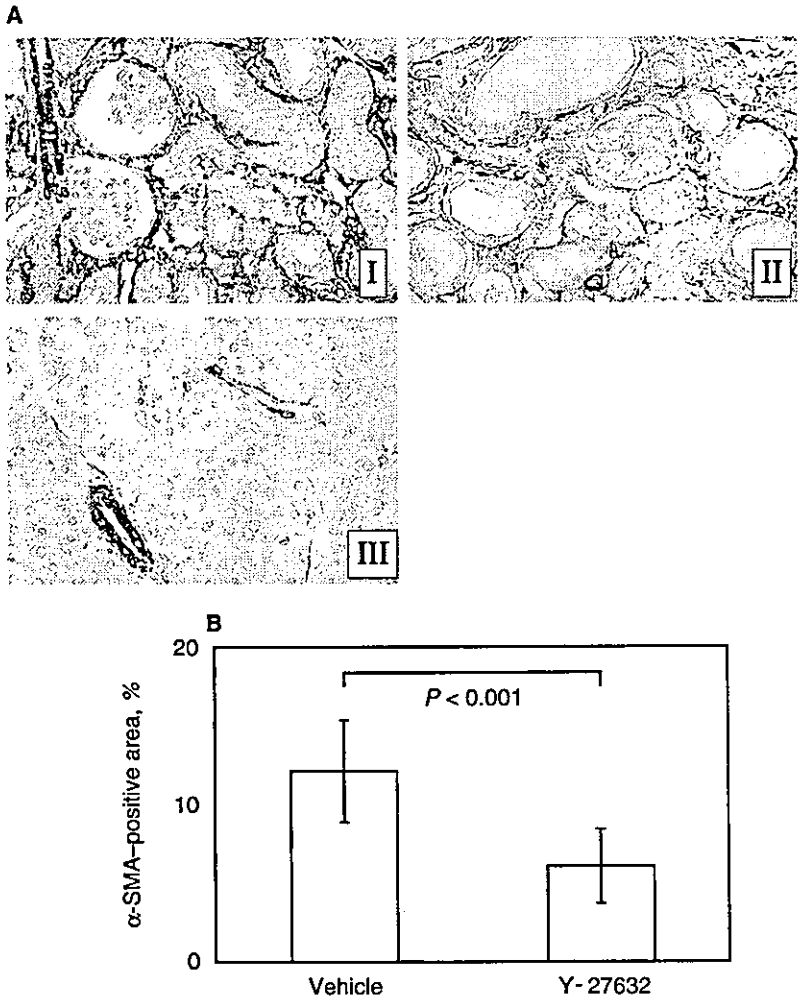

Fig. 3. Immunohistochemical detection and quantitative analysis of smooth muscle α actin (SMαA) in obstructed kidneys 10 days after surgery. (*A*) Light-field photomicrographs of the renal cortical region reacted with mouse monoclonal anti-SMαA antibody from (*I*) vehicle-treated and (*II*) Y-27632-treated mouse obstructed kidneys 10 days after ureteral obstruction and (*III*) contralateral kidneys. Sections were counterstained with methylgreen (×400). (*B*) The SMαA-positive area was quantified with a computer-aided image manipulator. Five animals were analyzed for each group and 10 randomly selected high power fields were quantitated and averaged to obtain the value for each animal.

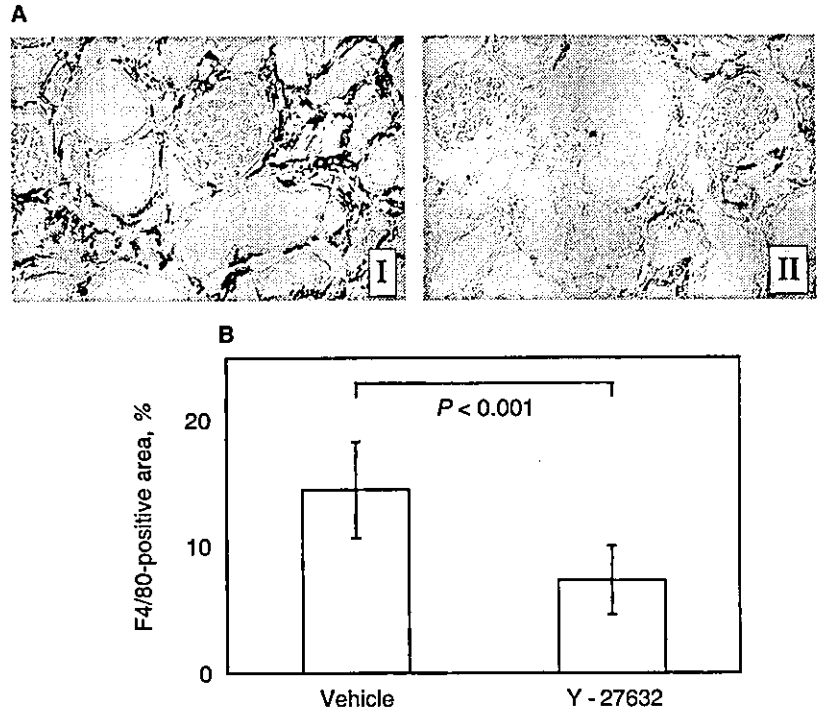

Fig. 4. Immunohistochemical detection and quantitative analysis of F4/80 in obstructed kidneys 10 days after surgery. (*A*) Light-field photomicrographs of the renal cortical region reacted with mouse monoclonal anti-F4/80 antibody from (*I*) vehicle-treated and (*II*) Y-27632-treated mouse obstructed kidneys 10 days after ureteral obstruction. Sections were counterstained with methylgreen (×400). (*B*) The F4/80-positive area was quantified with a computer-aided image manipulator. Five animals were analyzed for each group and 10 randomly selected high power fields were quantified, and averaged to obtain the value for each animal.

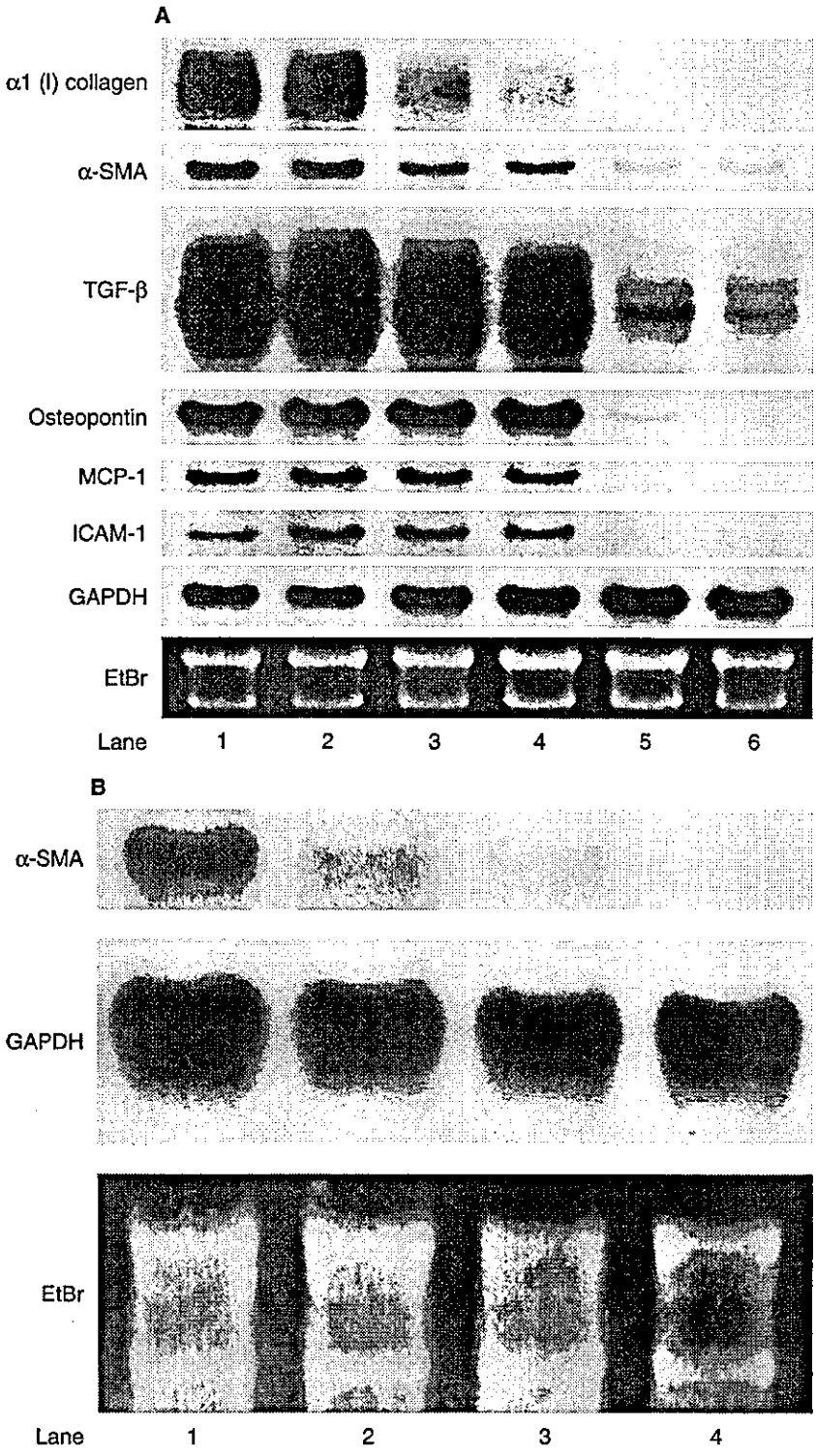

Fig. 5. mRNA expression in UUO mouse kidney 10 days after surgery and in mouse renal fibroblasts. (*A*) Representative results of Northern blotting of RNA from UUO mouse kidneys 10 days after surgery are shown. Each lane represents 20 μg of RNA from vehicle-treated obstructed kidneys (lanes 1 and 2), Y-27632-treated obstructed kidneys (lanes 3 and 4), and vehicle-treated contralateral kidneys (lanes 5 and 6). (*B*) Representative results of Northern blotting of RNA from mouse renal fibroblasts are shown. Each lane represents 10 μg of RNA treated with Y-27632 at 0 μmol/L (lane 1), 1 μmol/L (lane 2), 10 μmol/L (lane 3) or 100 μmol/L (lane 4).

functions of RhoB and RhoC are largely unknown compared with RhoA, it has been reported that RhoB was induced by PDGF and epidermal growth factor in rat fibroblast [34] and that RhoB regulates apoptosis [35]. It is also reported that overexpression of RhoC enhances tumor metastasis [36]. Since up-regulation of RhoB and RhoC possibly plays an important role in the progression of interstitial fibrosis in UUO kidney, it is important to

Table 2. mRNA expression in mouse kidneys 4 and 10 days after the onset of ureteral obstruction

	4 day			10 day		
	Vehicle	Y-27632	P	Vehicle	Y-27632	P
α1 (I) collagen	1 ± 0.184	0.705 ± 0.065	<0.05	1 ± 0.196	0.555 ± 0.224	<0.05
SMαA	1 ± 0.182	0.743 ± 0.074	<0.05	1 ± 0.130	0.587 ± 0.130	<0.005
TGF-β	1 ± 0.184	0.537 ± 0.095	<0.005	1 ± 0.167	0.523 ± 0.236	<0.01
Osteopontin	1 ± 0.159	0.891 ± 0.073		1 ± 0.080	0.866 ± 0.074	<0.05
MCP-1	1 ± 0.281	0.861 ± 0.111		1 ± 0.230	0.909 ± 0.199	
ICAM-1	1 ± 0.285	0.831 ± 0.101		1 ± 0.195	1.045 ± 0.176	

Data are: $N = 5$, mean ± SD. Relative induction of α1 (I) collagen, SMαA, osteopontin, MCP-1, ICAM-1 and TGF-β mRNA by densitometry of the Northern blotting autoradiograms. The densitometoric values of vehicle treated mice were taken as 1. Results are mean ± standard deviation of 5 independent animals.

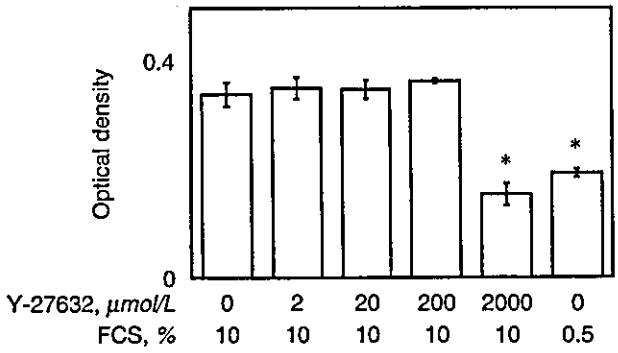

Fig. 6. Cell proliferation in mouse renal fibroblasts. Inhibitory effects of Y-27632 on proliferation of normal BDF1-derived renal fibroblasts (p9) as determined by MTT incorporation. Results are means ± SD of 5 independent experiments. $^*P < 0.001$ vs. vehicle-treated fibroblast.

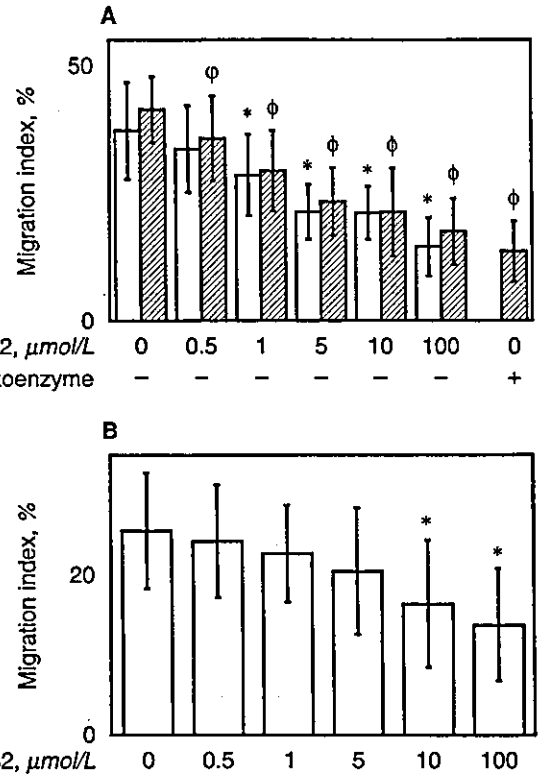

Fig. 7. Cell migration in mouse macrophages. (*A*) Inhibitory effects of Y-27632 on migration of RAW 264.7 mouse macrophages stimulated by MCP-1 at 2.5 ng/mL (□) and 25 ng/mL (▨). (*B*) Inhibitory effects of Y-27632 on migration of RAW 264.7 mouse macrophages stimulated by Ang II 1 μM (□). Results are means ± SD of 3 independent experiments. $^*P < 0.001$, $^\Phi P < 0.005$ and $^\phi P < 0.001$ vs. corresponding vehicle-treated macrophages.

elucidate how these signal transduction pathways affect in UUO kidney in detail.

In the present study, interstitial fibrosis in UUO kidneys was significantly reduced by Y-27632 administration, which was accompanied by suppression of both SMαA expression and macrophage infiltration. The appearance of SMαA-positive activated interstitial cells is one of the early changes leading to fibrosis in the tubulointerstitium. The enhanced expression of SMαA is a marker of interstitial phenotypic change in various forms of renal disease and these activated interstitial cells are called 'myofibroblasts' [37]. The appearance of myofibroblasts also has been considered to play a key role in the progression of renal fibrosis in interstitial lesions [29, 38]. In the present study, reduced SMαA expression was confirmed not only by immunohistochemical detection, but also by Northern blotting using whole kidneys and cultured renal fibroblasts. Recently, it was reported that smooth muscle differentiation marker gene expression is regulated by Rho-mediated actin polymerization and that Y-27632 administration inhibited the synthesis of SMαA isoform to a greater extent than the ubiquitously expressed β actin isoform [39]. These observations suggested that the Rho-ROCK signaling pathway plays an important role in the regulation of smooth muscle differentiation marker expression, while it plays a much less important role in the regulation of ubiquitously expressed genes such as non-muscle β actin. Moreover, it was reported that myofibroblast contraction is reduced by Y-27632 [40]. These findings are of interest because the appearance of myofibroblasts has also been considered to play a key role in the progression of fibrosis not only in the renal interstitium, but also in the renal glomerulus [29, 41], liver [42], lung [43] and pancreas [44],

which suggests that Y-27632 may be efficacious for progressive proliferative glomerulonephritis, hepatic fibrosis, interstitial pneumonitis and pancreatitis. In the contralateral kidney, positive staining for SMαA was seen only in the vascular smooth muscle cells, and Y-27632 treatment seemed to have no effect on these stainings.

Y-27632 suppressed TGF-β mRNA expression in vivo in the present study. Several reports have shown that TGF-β signaling is regulated by Rho [45–47] and our present data support these reports. Since the blockade of TGF-β signaling is known to suppress renal interstitial fibrosis in UUO model kidney [48], the effect of Y-27632 treatment might partly be due to suppression of TGF-β expression. In cultured fibroblast, reductions of neither α1(I) collagen nor TGF-β mRNA levels were not significant. The dissociation between in vivo experiment and in vitro one remains to be elucidated, but one possible explanation is as follows. In the development of renal interstitial fibrosis, tubular cells and infiltrated macrophages are supposed to play important roles by the influencing the surrounding renal fibroblasts. In Y-27632 treated kidney, Y-27632 might have indirectly affected renal fibroblasts through the inhibition of activated tubular cells and/or infiltrated macrophages, which resulted in the reduction of α1(I) collagen and TGF-β mRNA expressions in the in vivo experiment.

Macrophage infiltration, one of the key mechanisms involved in the progression of interstitial fibrosis, was suppressed by Y-27632. Several mechanisms seemed to be related to the reduction of macrophage infiltration. First, we examined the mRNA levels of the typical macrophage chemokines osteopontin, MCP-1 and ICAM-1 by Northern blotting because several reports suggested that Rho is closely related to the expression of ICAM-1 [49]. However, there were no significant reductions in the levels of expression of these genes in the Y-27632-treated group. Second, we studied the direct effect of Y-27632 on macrophage migration. The Rho signaling pathway is thought to be very important for cell migration as reviewed by Horwitz and Parsons [50]. It was reported that cell migration was down-regulated by blocking the Rho-ROCK signaling pathway by administration of Y-27632 in rat liver stellate cells [51], human glioma cells [52], human neutrophil [53] and human prostate cancer cells [54] human monocyte [55]. We demonstrated that Y-27632 inhibited migration of macrophages, and this observation may partly explain the significant attenuation of macrophage infiltration in Y-27632 treated mouse UUO kidneys. Moreover, we demonstrated that Ang II stimulated macrophage motility. An increased level of angiotensin II plays an important role in the development of tubulointerstitial fibrosis in UUO kidney and that angiotensin-converting enzyme inhibitor ameliorates the interstitial fibrosis and macrophage infiltration in UUO kidneys [13]. Considering these reports and our present data, it is possible that Ang II contributes to development of interstitial fibrosis by promoting the migration of macrophages.

The inhibitory effect of Y-27632 on cell proliferation is still controversial. In the present study, Y-27632 did not show any inhibitory effect on mouse renal fibroblast proliferation. It was also reported that Y-27632 did not inhibit the proliferation of FCS-stimulated human umbilical vein endothelial cells [56]. However, it has been reported that Y-27632 inhibited thrombin-stimulated DNA synthesis in rat aortic smooth muscle cell [57]. Ishizaki and colleagues reported that Y-27632 abolished stress fibers in Swiss 3T3 cells at 10 μmol/L, but the G1 to S phase transition and cytokinesis were little affected at this concentration and they were affected at concentrations as high as 100 μmol/L [26].

In summary, the results presented here indicated the effects of Y-27632 on interstitial fibrosis and myofibroblast expansion in mouse kidneys with unilateral ureteral obstruction. Interstitial fibrosis was significantly improved along with decreases in SMαA and F4/80 immunostaining. Northern blot analyses also indicated that α1 (I) collagen, SMαA and TGF-β mRNA expressions were suppressed by Y-27632. In addition, Y-27632 inhibited macrophage migration.

In conclusion, the Rho-ROCK system may play an important role in the development of tissue fibrosis and may be a new therapeutic target for preventing interstitial fibrosis in progressive renal disease.

ACKNOWLEDGMENT

We are grateful to Dr. M. Uehata (Mitsubishi Pharma Corporation, Kanagawa, Japan) for the generous supply of Y-27632.

Reprint requests Dr. Toshiki Moriyama, Department of Internal Medicine and Therapeutics (A8), Osaka University Graduate School of Medicine, 2-2 Yamadaoka, Suita Osaka 565-0871, Japan.
E-mail: moriyama@medone.med.osaka-u.ac.jp

REFERENCES

1. KLAHR S: New insights into the consequences and mechanisms of renal impairment in obstructive nephropathy. *Am J Kidney Dis* 18: 689–699, 1991
2. KLAHR S, PURKERSON ML: The pathophysiology of obstructive nephropathy: The role of vasoactive compounds in the hemodynamic and structural abnormalities of the obstructed kidney. *Am J Kidney Dis* 23:219–223, 1994
3. RICARDO S, DING G, EUFEMIO M, DIAMOND J: Antioxidant expression in experimental hydronephrosis: Role of mechanical stretch and growth factors. *Am J Physiol* 272:F789–F798, 1997
4. DIAMOND JR, KEES FD, DING G, *et al*: Macrophages, monocyte chemoattractant peptide-1, and TGF-beta 1 in experimental hydronephrosis. *Am J Physiol* 266(6Pt2):F926–F933, 1994
5. DIAMOND JR, KEES FD, RICARDO SD, *et al*: Early and persistent up-regulated expression of renal cortical osteopontin in experimental hydronephrosis. *Am J Pathol* 146:1455–1466, 1995
6. RICARDO SD, LEVINSON ME, DEJOSEPH MR, DIAMOND JR: Expression of adhesion molecules in rat renal cortex during experimental hydronephrosis. *Kidney Int* 50:2002–2010, 1996
7. MORIYAMA T, KAWADA N, AKAGI Y, *et al*: TCV-116 inhibits intersti-

tial fibrosis and HSP47 mRNA in rat obstructive nephropathy. *Kidney Int* 52(Suppl 63):S232–S235, 1997
8. Moriyama T, Kawada N, Ando A, *et al*: Up-regulation of HSP47 in the mouse kidneys with unilateral ureteral obstruction. *Kidney Int* 54:110–119, 1998
9. Schreiner GF, Harris KPG, Purkerson ML, Klahr S: Immunological aspects of acute ureteral obstruction: Immune cell infiltrate in the kidney. *Kidney Int* 34:487–493, 1988
10. Kaneto H, Morrissey J, Klahr S: Increased expression of TGF-beta 1 mRNA in the obstructed kidney of rats with unilateral ureteral ligation. *Kidney Int* 44:313–321, 1993
11. Diamond JR, van Goor H, Ding G, Engelmyer E: Myofibroblasts in experimental hydronephrosis. *Am J Pathol* 146:121–129, 1995
12. el Dahr S, Gee J, Dipp S, *et al*: Upregulation of renin-angiotensin system and downregulation of kallikrein in obstructive nephropathy. *Am J Physiol* 264(5 Pt 2):F874–F881, 1993
13. Kaneto H, Morrissey J, McCracken R, *et al*: Enalapril reduces collagen type IV synthesis and expansion of the interstitium in the obstructed rat kidney. *Kidney Int* 45:1637–1647, 1994
14. Reyes AA, Klahr S: Renal function after release of ureteral obstruction: Role of endothelin and the renal artery endothelium. *Kidney Int* 42:632–638, 1992
15. Kawada N, Moriyama T, Ando A, *et al*: Increased oxidative stress in mouse kidneys with unilateral ureteral obstruction. *Kidney Int* 56:1004–1013, 1999
16. Moriyama T, Kawada N, Nagatoya K, *et al*: Fluvastatin, an HMG-CoA reductase inhibitor, suppresses the oxidative stress and fibrosis in the interstitium of mouse kidneys with unilateral ureteral obstruction. *Kidney Int* 59:2095–2103, 2001
17. Madaule P, Axel R: A novel *ras*-related gene family. *Cell* 41:31–40, 1985
18. Ridley AJ, Hall A: The small GTP-binding protein rho regulates the assembly of focal adhesions and actin stress fiber in response to growth factors. *Cell* 70:389–399, 1992
19. Hirata K, Kikuchi A, Sasaki T, *et al*: Involvement of rho p21 in the GTP-enhanced calcium ion sensitivity of smooth muscle contraction. *J Biol Chem* 267:8719–8722, 1992
20. Mabuchi I, Hamaguchi Y, Fujimoto H, *et al*: A rho-like protein is involved in the organisation of the contractile ring in dividing sand dollar eggs. *Zygote* 1:325–331, 1993
21. Yamamoto M, Marui N, Sakai T, *et al*: ADP-ribosylation of the rhoA gene product by botulinum C3 exoenzyme causes Swiss 3T3 cells to accumulate in the G1 phase of cell cycle. *Oncogene* 8:1449–1455, 1993
22. Aoki H, Izumo S, Sadoshima J: Angiotensin II activates RhoA in cardiac myocytes: A critical role of RhoA in angiotensin II-induced premyofibril formation. *Circ Res* 82:666–676, 1998
23. Aikawa R, Komuro I, Nagai R, Yazaki Y: Rho plays an important role in angiotensin II-induced hypertrophic responses in cardiac myocytes. *Mol Cell Biochem* 212:177–182, 2000
24. Rankin S, Morii N, Narumiya S, Rozengurt E: Botulinum C3 exoenzyme blocks the tyrosine phosphorylation of p125FAK and paxillin induced by bombesin and endothelin. *FEBS Lett* 354:315–319, 1994
25. Uehata M, Ishizaki T, Satoh H, *et al*: Calcium sensitization of smooth muscle mediated by a Rho-associated protein kinase in hypertension. *Nature* 389:990–994, 1997
26. Ishizaki T, Uehata M, Tamechika I, *et al*: Pharmacological properties of Y-27632, a specific inhibitor of Rho-associated kinases. *Mol Pharmacol* 57:976–983, 2000
27. Muller GA, Markovic-Lipkovski J, Rodemann HP: The progression of renal disease: On the pathogenesis of renal interstitial fibrosis. *Klin Wochenschr* 69:576–586, 1991
28. Chomczynski P, Sacchi N: Single-step method of RNA isolation by acid guanidinium thiocyanate-phenol-chloroform extraction. *Anal Biochem* 162:156–159, 1987
29. Ando Y, Moriyama T, Oka K, *et al*: Enhanced interstitial expression of caldesmon in IgA nephropathy and its suppression by glucocorticoid-heparin therapy. *Nephrol Dial Transplant* 14:1408–1417, 1999
30. Hansen MB, Nielsen SE, Berg K: Re-examination and further development of a precise and rapid dye method for measuring cell growth/cell kill. *J Immunol Methods* 119:203–210, 1989
31. Ikeda K, Wakahara T, Wang YQ, *et al*: *In vitro* migratory potential of rat quiescent hepatic stellate cells and its augmentation by cell activation. *Hepatology* 29:1760–1767, 1999
32. Nath KA: Tubulointerstitial changes as a major determinant in the progression of renal damage. *Am J Kidney Dis* 20:1–17, 1992
33. Couser WG, Johnson RJ: Mechanisms of progressive renal disease in glomerulonephritis. *Am J Kidney Dis* 23:193–198, 1994
34. Jahner D, Hunter T: The ras-related gene RhoB is an immediate-early gene inducible by V-Fps, epidermal growth factor, and platelet-derived growth factor in rat fibroblasts. *Mol Cell Biol* 11:3682–3690, 1991
35. Fritz G, Kaina B: Ras-related GTPase RhoB forces alkylation-induced apoptotic cell death. *Biochem Biophys Res Commun* 268: 784–789, 2000
36. Clark EA, Golub TR, Lander ES, Hynes RO: Genomic analysis of metastasis reveals an essential role for RhoC. *Nature* 406:532–535, 2000
37. Goumenos DS, Brown CB, Shortland J, Elahas AM: Myofibroblasts, predictor of progression of mesangial IgA nephropathy? *Nephrol Dial Transplant* 9:1418–1425, 1994
38. Hewitson D, Wu L, Becker GJ: Interstitial myofibroblasts in experimental renal infection and scarring. *Am J Nephrol* 15:411–417, 1995
39. Mack CP, Somlyo AV, Hautmann M, *et al*: Smooth muscle differentiation marker gene expression is regulated by RhoA-mediated actin polymerization. *J Biol Chem* 276:341–347, 2001
40. Parizi M, Howard EW, Tomasek JJ: Regulation of LPA-promoted myofibroblast contraction: Role of Rho, myosin light chain kinase, and myosin light chain phosphatase. *Exp Cell Res* 254:210–220, 2000
41. Utsunomiya Y, Kawamura T, Abe A, *et al*: Significance of mesangial expression of α-smooth muscle actin in the progression of IgA nephropathy. *Am J Kidney Dis* 34:902–910, 1999
42. Friedman SL: The cellular basis of hepatic fibrosis: mechanisms and treatment strategies. *N Engl J Med* 328:1828–1835, 1993
43. Vyalov SL, Gabbiani G, Kapanci Y: Rat alveolar myofibroblast acquire alpha-smooth muscle actin expression during bleomycin-induced-pulmonary fibrosis. *Am J Pathol* 143:1754–1765, 1993
44. Suda K, Takase M, Takei K, *et al*: Histopathologic and immunohistochemical studies on the mechanism of interlobular fibrosis of the pancreas. *Arch Pathol Lab Med* 124:1302–1305, 2000
45. Choi SE, Choi EY, Kim PH, Kim JH: Involvement of protein kinase C and Rho GTPase in the nuclear signalling pathway by transforming growth factor-beta1 in rat-2 fibroblast cells. *Cell Signal* 11:71–76, 1999
46. Park HJ, Galper JB: 3-Hydroxy-3-methylglutaryl CoA reductase inhibitors up-regulate transforming growth factor-beta signaling in cultured heart cells via inhibition of geranylgeranylation of RhoA GTPase. *Proc Natl Acad Sci USA* 96:11525–11530, 1999
47. Kim SI, Kim HJ, Han DC, Lee HB: Effect of lovastatin on small GTP binding proteins and on TGF-beta1 and fibronectin expression. *Kidney Int* (Suppl 77):S88–S92, 2000
48. Isaka Y, Tsujie M, Ando Y, *et al*: Transforming growth factor-β1 antisense oligodeoxynucleotides block interstitial fibrosis in unilateral ureteral obstruction. *Kidney Int* 58:1885–1892, 2000
49. Tominaga T, Sugie K, Hirata M, *et al*: Inhibition of PMA-induced, LFA-1-dependent lymphocyte aggregation by ADP ribosylation of the small molecular weight GTP binding protein, rho. *J Cell Biol* 120:1529–1537, 1993
50. Horwitz AR, Parsons JT: Cell migration—Movin' on. *Science* 286:1102–1103, 1999
51. Kawada N, Seki S, Kuroki T, Kaneda K: ROCK inhibitor Y-27632 attenuates stellate cell contraction and portal pressure increase induced by endothelin-1. *Biochem Biophys Res Commun* 266:296–300, 1999
52. Manning TJJ, Parker JC, Sontheimer H: Role of lysophosphatidic acid and rho in glioma cell motility. *Cell Motil Cytoskelton* 45:185–199, 2000
53. Niggli V: Rho-kinase in human neutrophils: A role in signalling for myosin light chain phosphorylation and cell migration. *FEBS Lett* 445:69–72, 1999
54. Somlyo AV, Bradshaw D, Ramos S, *et al*: Rho-kinase inhibitor

retards migration and in vivo dissemination of human prostate cancer cells. *Biochem Biophys Res Commun* 269:652–659, 2000
55. ASHIDA N, ARAI H, YAMASAKI M, KITA T: Distinct signaling pathways for MCP-1-dependent integrin activation and chemotaxis. *J Biol Chem* 276:16555–16560, 2001
56. UCHIDA S, WATANABE G, SHIMADA Y, *et al*: The suppression of small GTPase Rho signal transduction pathway inhibits angiogenesis *in vitro* and *in vivo*. *Biochem Biophys Res Commun* 269:633–640, 2000
57. SEASHOLTZ TM, MAJUMDAR M, KAPLAN DD, BROWN JH: Rho and Rho kinase mediate thrombin-stimulated vascular smooth muscle cell DNA synthesis and migration. *Circ Res* 84:1186–1193, 1999

Kidney International, Vol. 61 (2002), pp. 1853–1858

Role of uteroglobin G38A polymorphism in the progression of IgA nephropathy in Japanese patients

ICHIEI NARITA, NORIKO SAITO, SHIN GOTO, SONG JIN, KENTARO OMORI, MINORU SAKATSUME, and FUMITAKE GEJYO

Division of Clinical Nephrology and Rheumatology, Niigata University Graduate School of Medical and Dental Sciences 1-757, Asahimachi-dori, Niigata, 951-8510, Japan

Role of uteroglobin G38A polymorphism in the progression of IgA nephropathy in Japanese patients.

Background. Uteroglobin is a multifunctional protein and both its gene knockout and antisense transgenic mouse models develop the pathological and clinical features of IgA nephropathy. A genetic polymorphism in uteroglobin has been reported to be associated with progression of IgA nephropathy in a Caucasian population, but the findings remain controversial.

Methods. Genomic DNA was isolated from 595 individuals including 239 patients with IgAN, 160 patients with glomerulonephritis distinct from IgAN, and 196 healthy controls. The uteroglobin G38A genotype was determined by PCR-RFLP with *Sau*96I. To examine the possible association of uteroglobin gene polymorphism in the patients with and without IgAN, the uteroglobin genotype and allele frequency were compared between the two groups. In addition, associations between the polymorphism and blood pressure, proteinuria and prognosis of renal function were analyzed in the patients with IgAN to investigate the role of this gene polymorphism in the risk of progressive renal dysfunction in IgAN patients.

Results. The Cox proportional hazard regression model revealed that hypertension and proteinuria at the time of renal biopsy were independent risk factors for poor renal survival. Uteroglobin genotype was not significantly associated with the renal survival rate. However, in the patients with heavy proteinuria (more than 2 g/day) or in those with hypertension at the time of renal biopsy, the renal survival of patients with the GG genotype was significantly worse than the other genotypes.

Conclusion. Uteroglobin GG genotype may be a genetic marker for rapid disease progression to end-stage renal failure, especially in the IgAN patients with heavy proteinuria or high blood pressure.

Immunoglobulin A nephropathy (IgAN), one of the most prevalent forms of primary glomerulonephritis, is the major course of end-stage renal failure [1]. The disease has a variable clinical course and one third of the patients with IgAN progress to end-stage renal disease (ESRD) within 10–20 years of the onset [2–4]. The pathogenesis of mesangial IgA deposition and the mechanism of inter-individual differences in the rate of disease progression are still unclear [5]. An accumulating amount of evidence suggests that genetic factors determine the susceptibility to developing IgAN as well as to the progression of renal dysfunction [6, 7]. For the purpose of better understanding both the pathogenesis and the mechanism of IgAN progression, it is thought to be important to identify the genetic background for the susceptibility both to IgAN and to ESRD. Poor prognostic factors in clinical findings have been identified as high blood pressure, severe proteinuria, and a severe histological appearance of the renal biopsy [4, 8].

Uteroglobin is mainly produced by mucosal epithelial cells and is present in both blood and urine [9, 10]. Uteroglobin is an evolutionarily conserved, steroid-inducible, homodimeric molecule. It is a secreted protein with many functions and potent immunomodulatory/anti-inflammatory properties [11]. Uteroglobin has a high affinity for fibronectin and forms fibronectin-uteroglobin heterodimers, which counteract the fibronectin-collagen interactions required for abnormal deposits [12]. The generation of uteroglobin knockout mice has revealed that disruption of this gene causes severe renal disease due to abnormal deposits of fibronectin and collagen in the glomeruli, as well as a lack of polychlorinated biphenyl binding and increased oxygen toxicity [13].

Thus, uteroglobin may be a good candidate for genetic backgrounds, which influence the development and progression of IgAN. In fact, an association between genetic polymorphism of uteroglobin and the rate of progression, but not the development of disease, has been reported in patients with IgAN from a Caucasian population [14, 15]. However, the results of these previous reports still remain controversial. The purpose of this study was to investigate the role of uteroglobin G38A polymor-

Key words: IgA nephropathy, gene polymorphism, progressive renal disease, end-stage renal disease, proteinuria, glomerulonephritis.

Received for publication September 19, 2001
and in revised form December 4, 2001
Accepted for publication December 24, 2001

© 2002 by the International Society of Nephrology

phism in the development of IgAN, as well as in the survival of renal function in Japanese patients with IgA nephropathy.

METHODS

The ethics committee of the institution involved approved the protocol for the study and informed written consent for the genetic studies was obtained from all participants. Genomic DNA of peripheral blood cells was isolated by an automatic DNA isolation system (NA-1000; Kurabo, Osaka, Japan) from 595 Japanese individuals including 239 patients with histologically confirmed IgAN. Henoch-Schönlein purpura and secondary IgAN such as hepatic glomerulosclerosis were excluded from the analysis.

Diagnosis of IgAN was based on a kidney biopsy that revealed the presence of dominant or co-dominant glomerular mesangial deposits of IgA as assessed by an immunofluorescence examination. The others consist of 160 patients with renal diseases which were confirmed histologically to have no mesangial IgA deposition, including 45 mesangial proliferative glomerulonephritis without mesangial IgA deposition, 32 membranous nephropathy, 19 minor glomerular abnormality, 9 mesangioproliferative glomerulonephritis, 8 thin basement membrane disease, 6 nephrosclerosis, 4 focal segmental glomerulonephritis, and 37 other renal diseases (diabetic nephropathy, donor for kidney transplantation, primary amyloidosis, and Alport syndrome, and other). The mean age was 37.1 years old in patients with IgAN and 39.2 in those with other glomerulonephritis.

Clinical characteristics of the patients with IgAN including age, sex, duration of observation (in months), level of urinary protein excretion (g/day), serum creatinine (S_{Cr}; mg/dL), and 24-hour creatinine clearance (mL/min) were investigated. Hypertension was defined by the use of one or more antihypertensive medications and/or a blood pressure greater than or equal to 140 mm Hg systolic or 90 mm Hg diastolic. The primary end point, end-stage renal disease (ESRD), was defined as the date at which the S_{Cr} levels doubled after the time of diagnosis, or when patients underwent their first hemodialysis.

The administrations of glucocorticoids, antihypertensive agents, and angiotensin-converting enzyme (ACE) inhibitors also were recorded for each patient.

To provide the control of local genotype frequency being examined, 196 Japanese volunteers (97 female and 99 male) with no history of renal disease or hypertension were recruited also.

Determination of the genotypes

We studied a single nucleotide polymorphism G38A in the uteroglobin gene, which is located downstream from the transcription-initiation site within the noncoding region of exon 1. This polymorphism was reported to be associated with a predisposition to asthma and with the progression of IgAN in a Caucasian population [14–16]. Polymerase chain reaction (PCR) of the genomic DNA was performed to amplify a 258-bp fragment in exon 1 of the uteroglobin gene using the primer pair 5′-CAG TAT CTT ATG TAG AGC CC-3′ and 5′-CCT GAG AGT TCC TAA GTC CAG G-3′. The reaction mixture contained 1 × PCR buffer, 1.5 mmol/L $MgCl_2$, 200 mmol/L deoxynucleotide triphosphates (dNTPs), 1 unit Taq DNA polymerase (Takara, Kyoto, Japan), 10 pmol of each primer, and 50 to 100 ng genomic DNA. The PCR amplification reaction consisted of a cycle at 95°C for five minutes, followed by 35 cycles of denaturation at 94°C for 15 seconds, annealing at 58°C for 15 seconds, and extension at 72°C for 30 seconds. A final extension was performed at 72°C for five minutes. The PCR products were digested with restriction endonuclease *Sau96I* (New England Biolabs Inc., Beverly, MA, USA), and electrophoresed on 3% agarose gel. For 38G alleles, this resulted in a 128-bp and a 130-bp fragment, whereas the 258-bp 38A alleles lacked its restrictive site.

Statistical analysis

Statview 5.0 statistical software (Abacus Concepts, Inc. Berkeley, CA, USA) was used for statistical analyses on a Macintosh G4 computer. Chi-square analysis was used when comparing allele frequencies and categorical variables between the groups. Hardy-Weinberg equilibrium was tested by a Chi-square test with 1 *df*. The Kaplan-Meier method and the Cox proportional hazards regression model analyzed the time course from renal biopsy to end point (initiation of dialysis or a doubling in the S_{Cr} level after the time of diagnosis). Covariates were selected by a stepwise backward method and the effects of these covariates were expressed by a hazard ratio. *P* less than 0.05 was considered statistically significant.

RESULTS

The 595 subjects consisting of 239 patients with histologically proven IgAN, 160 with other glomerulonephritis distinct from IgAN, and 196 healthy controls were genotyped for uteroglobin G38A. Table 1 lists the genotype distribution and the allele frequency of this gene polymorphism in these groups. The allele frequency of 38G in uteroglobin for the Japanese population was 0.585 (0.592 in IgAN patients, 0.563 in the patients with other glomerulonephritis, and 0.594 in the controls). These numbers were not statistically different between the patients with IgAN and those with other types of glomerulonephritis. Moreover, no difference was recognized in the genotype and allele frequency between the patients with either IgAN or other glomerulonephritis and healthy controls. The expected frequency of the genotypes in

Table 1. Frequencies of genotypes and alleles of the uteroglobin G38A gene polymorphism in patients with IgA nephropathy, those with other glomerulonephritis, and controls without renal disease

	IgAN $N=239$	Other GN $N=160$	Control $N=196$	χ^2	P value	
Genotype						
AA	43	28	32			
AG	109	84	95	1.086	0.298	(IgAN vs. other GN)
GG	87	48	69	0.237	0.888	(GN vs. controls)
Allele						
A	0.408	0.437	0.406	0.687	0.407	(IgAN vs. other GN)
G	0.592	0.563	0.594	0.827	0.363	(GN vs. controls)

Abbreviations are: IgAN, IgA nephropathy; GN, glomerulonephritis.

Table 2. Clinical characteristics of patient with IgA nephropathy

	All patients $N=239$	GG $N=87$	AG/AA $N=152$	P
Male sex %	46.4	51.7	43.4	NS
At the time of renal biopsy				
Age *years*	37.1 ± 13.6	35.5 ± 13.2	38.0 ± 13.8	NS
U protein *g/day*	1.3 ± 1.3	1.3 ± 1.3	1.4 ± 1.3	NS
S_{Cr} *mg/dL*	1.0 ± 0.6	1.1 ± 0.9	1.0 ± 0.4	NS
C_{Cr} *mL/min*	86.6 ± 31.0	85.5 ± 33.3	87.2 ± 29.7	NS
Blood pressure *mm Hg*				
Systolic	128.1 ± 18.4	129.2 ± 17.6	128.8 ± 16.4	NS
Diastolic	77.2 ± 13.3	78.0 ± 12.4	77.3 ± 10.9	NS
Hypertension %	40.6	56.3	31.6	0.072
During the observation				
Observed periods *months*	95.8 ± 66.8	93.7 ± 72.4	96.6 ± 63.5	NS
ESRD %	35.1	41.3	31.5	NS
Treatment				
Glucocorticoid %	30.3	27.1	31.2	NS
Anti-HT drugs %	62.2	66.1	59.8	NS
ACEI %	50.0	44.0	53.8	NS

Abbreviations are: U protein, urinary protein; S_{Cr}, serum creatinine; C_{Cr}, creatinine clearance; ESRD, end-stage renal disease; anti-HT drug, antihypertensive drug; ACEI, angiotensin I converting enzyme inhibitor.

each group, under the assumption of Hardy-Weinberg equilibrium, did not differ from the observed genotype frequencies.

Clinical characteristics of the patients with IgAN are listed in Table 2. A comparison between patients either homozygous or heterozygous for A allele and those with the GG genotype showed no significant differences in age, sex, S_{Cr}, creatinine clearance (C_{Cr}), blood pressure at the time of renal biopsy, or in the percentage of cases treated by ACE inhibitors. The incidence of hypertension in the patients with GG genotype tended to be higher than that in those with other genotypes, although the difference was not statistically significant ($P = 0.072$).

Among all patients with IgAN ($N = 239$), 84 (35.1%) progressed to ESRD during the mean follow-up duration of 95.8 ± 66.8 months. The Cox proportional hazard regression (HR) model indicated proteinuria level of more than 2 g/day (HR = 3.671, 95% CI, 2.19 to 6.16; $P < 0.0001$) and hypertension (HR = 2.407, 95% CI, 1.22 to 3.45; $P = 0.007$) were independent risk factors for progression to ESRD (Table 3). These covariates were selected by stepwise backward analysis. Therapeutic agents such as glucocorticoids, antihypertensives, or ACE inhibitors were not selected as a significant prognostic factor by this analysis. The genotype of uteroglobin G38A polymorphism did not significantly affect the prognosis of renal function (GG vs. AG/AA; HR = 1.327, 95% CI, 0.828 to 2.126, $P = 0.240$ by univariate analysis). In addition, the renal survival rate was not significantly different between the two groups (Kaplan-Meier, $\chi^2 = 3.560$, $P = 0.059$; Fig. 1). The GG genotype was present in a numerically greater proportion of patients with ESRD, but the difference was not statistically significant (OR, 1.53; $P = 0.083$).

Next, the role of uteroglobin G38A polymorphism on the renal survival in the stratified patients with or without hypertension at the time of renal biopsy was examined (Fig. 2). In the patients with hypertension ($N = 97$), the renal survival of patients with the uteroglobin GG genotype was significantly worse than with other genotypes (Kaplan-Meier, $\chi^2 = 4.320$, $P = 0.038$, Fig. 2A), whereas no such difference was observed in the patients without hypertension (Kaplan-Meier, $\chi^2 = 0.071$, $P = 0.790$, Fig. 2B).

Table 3. Cox proportional hazards regression model

Variable	*P* value	HR	95% CI
U protein			
>2.0 g/day	<0.0001	3.671	2.19–616
<1.0 g/day	0.054	0.535	0.28–1.01
HT at the time of renal biopsy	0.007	2.047	1.22–3.45

Abbreviations are: HR, hazard ratio; U protein, urinary protein; HT, hypertension.

We also examined the effect of uteroglobin G38A polymorphism in the subgroup of patients with a proteinuria level of more than 2 g/day at the time of renal biopsy because the Cox proportional hazard regression model indicated that more than 2 g/day of proteinuria was a significant risk factor for progression to ESRD. In this analysis the renal survival of patients with the GG genotype was significantly poorer than with other genotypes (Kaplan-Meier, χ^2 = 6.030, P = 0.014; Fig. 3A). The 50% survival time in patient with the GG genotype was significantly shorter than that of the others (GG vs. GA/AA; 61.0 ± 12.8 months vs. 96.0 ± 13.0 months). This effect of uteroglobin G38A polymorphism was not detected in the patients with a proteinuria level of less than 2 g/day at the time of renal biopsy (Kaplan-Meier, χ^2= 0.015, P = 0.903; Fig. 3B).

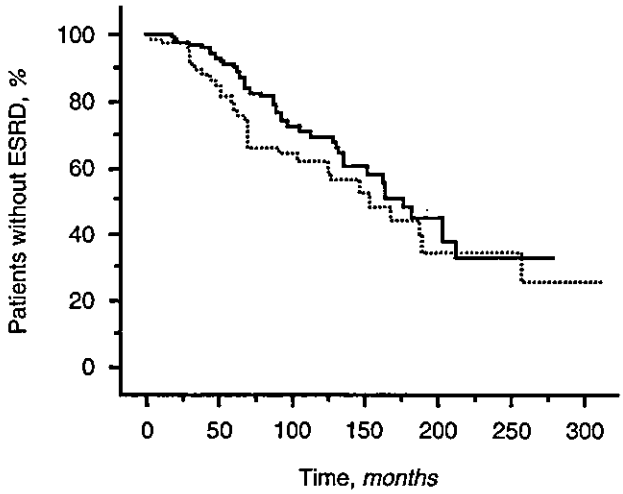

Fig. 1. Renal survival in IgA nephropathy patients with the GG (dashed line; N = 87) and with AG/AA genotypes (solid line; N = 152) of uteroglobin G38A polymorphism. Kaplan-Meier, log rank test, P = 0.059.

DISCUSSION

Uteroglobin is an attractive candidate for the genetic study of IgAN development, because both its gene knockout and its antisense transgenic mouse models developed the pathological features of IgAN [2, 12, 17]. However, the results of our study show that the genotype and allele frequencies of uteroglobin G38A polymorphism were not different between the patients with IgAN and those with other glomerulonephritis distinct from IgAN, indicating that the genetic polymorphism investigated has no involvement in the development of IgAN. This result is consistent with that of the previous studies in Caucasian populations [14, 15].

To investigate the risk factors for progression to ESRD, this study design employed a time-to-event approach rather than an analysis of mean slope of renal function, because a substantial proportion of our patients had stable or slowly declining renal function. In fact, only one-third of the patients progressed to the end point during the follow-up period in this study. It has been suggested that an analysis of mean slope of renal function is favored if a negligible proportion of patients have stable or slowly declining renal function [18].

The significant and interesting finding in this study is the effects of the G38A polymorphism in the uteroglobin gene on the rate of IgAN disease progression, which were observed only in the stratified groups of patients with hypertension and in those with heavy proteinuria (>2 g/day). These factors were shown to be independent risk factors for poor renal survival in our patients using the Cox proportional hazard regression model. The uteroglobin G38A polymorphism has no association with these risk factors themselves. If anything, the renal prognosis of the high-risk IgAN patients is further deteriorated when accompanied by the GG genotype. Thus, the genetic polymorphism in uteroglobin may have an influence on the sensitivity to these clinical risk factors.

Our present study could not detect a significant effect of uteroglobin G38A polymorphism on the disease progression in any of the patients, although a previous study showed that the GG genotype of G38A uteroglobin polymorphism was more common in patients with progression [15]. This may be due to a difference in the frequency of the uteroglobin G38 allele within the analyzed population, as the G38 allele frequency was lower in the Japanese population than in the Caucasian (0.585 vs. 0.682, respectively). Racial differences in allele frequencies might contribute to the conflicting results in association studies. Single nucleotide polymorphisms with high allele frequencies were reported to be more statistically informative than those with low allele frequencies in association studies [19].

There is also the possibility that patients with normal blood pressure and mild proteinuria are more frequent in this study, which may be due to a difference in the indication criteria of the renal biopsy. In fact, the mean blood pressure is lower in this study than in the previous report, although there was no difference in the mean value of the urinary protein excretion. In addition, the difference in therapeutic strategy may have an influence

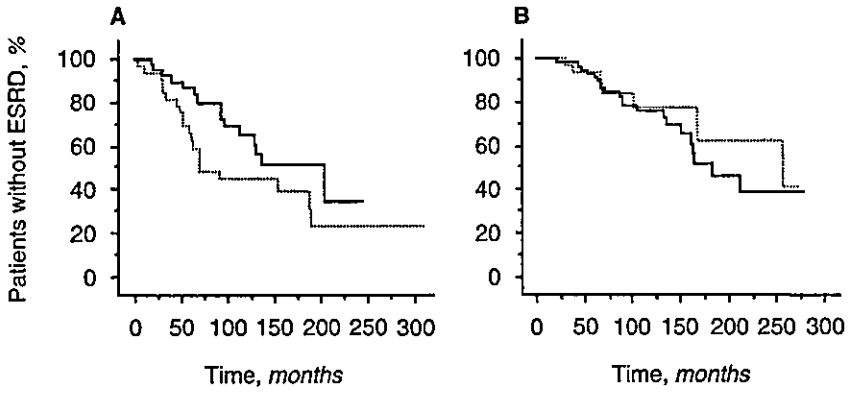

Fig. 2. Renal survival in IgA nephropathy patients with (*A*, Kaplan-Meier, log rank test, $P = 0.038$) and without (*B*, Kaplan-Meier, log rank test, $P = 0.790$) hypertension at the time of renal biopsy. Symbols are: (dotted line) GG genotype; (solid line) AG/AA genotype. In hypertensive patients (A), $N = 49$ GG genotype and 48 AG/AA genotype. In IgA nephropathy patients without hypertension (B), $N = 38$ GG genotype and 104 AG/AA genotype.

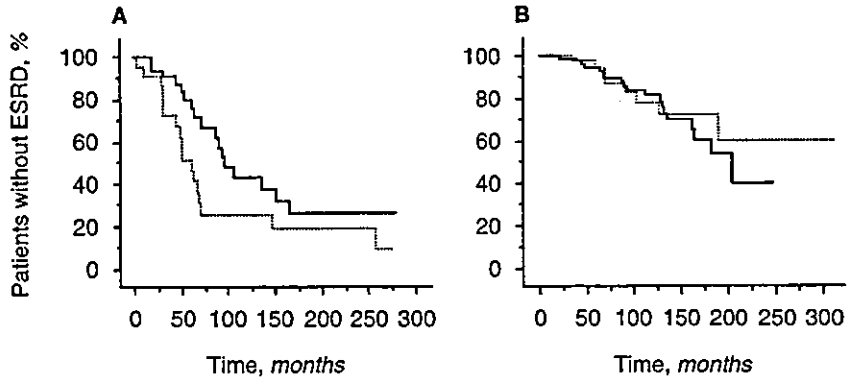

Fig. 3. Renal survival in IgA nephropathy patients with (*A*, Kaplan-Meier, log rank test, $P = 0.014$) and without (*B*, Kaplan-Meier, log rank test, $P = 0.903$) a proteinuria level of more than 2 g/day at the time of renal biopsy. Symbols are: (dotted line) GG genotype; (solid line) AG/AA genotype. In the patients with >2 g/day proteinuria (A), $N = 29$ GG genotype and 49 AG/AA genotype. In patients with ≤2 g/day proteinuria (B), $N = 58$ GG genotype and 103 AG/AA genotype.

on the role of genetic polymorphism in disease progression. In the present study 30.3% of the patients were treated with glucocorticoids, although no information about the glucocorticoid therapy in the previous report is available.

The exact mechanism by which the uteroglobin G38A polymorphism affects only the patients at a high risk for the progression to ESRD is unclear.

In the previous report, Szelestei et al mentioned that they could not exclude a blood pressure-effect for the association of the uteroglobin polymorphism and disease progression of IgAN [15]. The incidence of hypertension in the patients with GG genotype also tended to be higher (but not statistically significant) than that in those with other genotypes in this study. It is known that uteroglobin is a remarkable functional protein, and that transgenic mice that have been rendered deficient and humans who have been characterized as deficient in this protein exhibit tendencies toward inflammatory, fibrotic, and oncologic diseases, demonstrating the potential of this protein as a therapeutic agent [20]. The polymorphism at the 5′ untranslated region of exon 1 in this gene has been shown to directly affect the expression of uteroglobin, although the gene construct with A at the 38th site showed a rather decreased activity compared to that showed by the G gene construct [14]. The results of our study suggests that high blood pressure or heavy proteinuria affects the level of uteroglobin, because the genetic polymorphism investigated in here has been reported to affect the promoter activity of this gene. It is likely that uteroglobin has substantial biological effects on renal cells in vitro and in vivo, although we have no data or knowledge to prove this opinion. The mechanism(s) of uteroglobin action is likely to be even more complex as it also functions via a putative receptor-mediated pathway that is yet to be clearly defined.

The limitation of this study is that the association between the level of uteroglobin and the disease progression is not available. We have no data for the expression of uteroglobin in the kidney. Further study is required to clarify the functional mechanism of the role of this gene polymorphism. It is essential to elucidate the molecular mechanism of uteroglobin's functions in both physiological and pathological situations.

Many studies of genetic factors for susceptibility or progression of IgAN have been published, although no positive or negative association of these genetic candidates are useful for diagnostic or therapeutic purposes. They include genes for human lymphocyte antigens (HLA),

complement, renin-angiotensin system, IgA immune system, etc. [21].

In conclusion, these results demonstrate that the uteroglobin G38A polymorphism affects the disease progression of IgAN especially in patients with hypertension and heavy proteinuria, which are clinical risk factors for progression to ESRD. This indicates that antihypertensive treatment and glucocorticoid treatment should be administered more extensively to the patients with GG genotype. Moreover, patients with both the GG genotype of uteroglobin and clinical risk factors such as hypertension and heavy proteinuria might be good candidates for new therapeutic strategies such as an uteroglobin-based therapy.

It is thought to be important to select the appropriate class of antihypertensive agents according to the characteristics of the patients including—if the evidence is available—a genetic marker such as uteroglobin G38A. However, we have no data to answer this matter. Moreover, we cannot completely exclude the possibility that some biases existed in the population analyzed here, because the sample size of each stratified group was not sufficiently large. To confirm the findings in our study, further investigation in a prospective trial with a large-scale population will be needed.

ACKNOWLEDGMENTS

This work was supported by a Grant-in-Aid for Scientific Research on Priority Areas (C) "Medical Genome Science," Grant-in-Aid for Scientific Research (C) from the Ministry of Education, Science, Sports and Culture of Japan, and by a grant from Sumitomo Pharmaceutical Co. We gratefully acknowledge the excellent technical assistance of Naofumi Imai, Satomi Takeuchi and Keiko Yamagiwa.

Reprint requests to Ichiei Narita, M.D., Division of Clinical Nephrology and Rheumatology, Niigata University Graduate School of Medical and Dental Sciences, 1-757, Asahimachi-dori, Niigata 951-8510, Japan. E-mail: naritai@med.niiagta-u.ac.jp

REFERENCES

1. Levy M, Berger J: Worldwide perspective of IgA nephropathy. *Am J Kidney Dis* 12:340–347, 1988
2. Koyama A, Igarashi M, Kobayashi M: Natural history and risk factors for immunoglobulin A nephropathy in Japan. Research Group on Progressive Renal Diseases. *Am J Kidney Dis* 29:526–532, 1997
3. Galla JH: IgA nephropathy. *Kidney Int* 47:377–387, 1995
4. Szeto CC, Lai FM, To KF, *et al*: The natural history of immunoglobulin a nephropathy among patients with hematuria and minimal proteinuria. *Am J Med* 110:434–437, 2001
5. Rantala I, Mustonen J, Hurme M, *et al*: Pathogenetic aspects of IgA nephropathy. *Nephron* 88:193–198, 2001
6. Scolari F, Amoroso A, Savoldi S, *et al*: Familial clustering of IgA nephropathy: Further evidence in an Italian population. *Am J Kidney Dis* 33:857–865, 1999
7. Hsu SI, Ramirez SB, Winn MP, *et al*: Evidence for genetic factors in the development and progression of IgA nephropathy. *Kidney Int* 57:1818–1835, 2000
8. Alamartine E, Sabatier JC, Guerin C, *et al*: Prognostic factors in mesangial IgA glomerulonephritis: An extensive study with univariate and multivariate analyses. *Am J Kidney Dis* 18:12–19, 1991
9. Atger M, Savouret JF, Milgrom E: Synthesis, purification and characterization of a DNA complementary to uteroglobin messenger RNA. *J Steroid Biochem* 13:1157–1162, 1980
10. Aoki A, Pasolli HA, Raida M, *et al*: Isolation of human uteroglobin from blood filtrate. *Mol Hum Reprod* 2:489–497, 1996
11. Mukherjee AB, Kundu GC, Mantile-Selvaggi G, *et al*: Uteroglobin: A novel cytokine? *Cell Mol Life Sci* 55:771–787, 1999
12. Zheng F, Kundu GC, Zhang Z, *et al*: Uteroglobin is essential in preventing immunoglobulin A nephropathy in mice. *Nat Med* 5: 1018–1025, 1999
13. Mukherjee AB, Kundu GC, Mandal AK, *et al*: Uteroglobin: Physiological role in normal glomerular function uncovered by targeted disruption of the uteroglobin gene in mice. *Am J Kidney Dis* 32:1106–1120, 1998
14. Kim YS, Kang D, Kwon DY, *et al*: Uteroglobin gene polymorphisms affect the progression of immunoglobulin A nephropathy by modulating the level of uteroglobin expression. *Pharmacogenetics* 11:299–305, 2001
15. Szelestei T, Bahring S, Kovacs T, *et al*: Association of a uteroglobin polymorphism with rate of progression in patients with IgA nephropathy. *Am J Kidney Dis* 36:468–473, 2000
16. Choi M, Zhang Z, Ten Kate LP, *et al*: Human uteroglobin gene polymorphisms and genetic susceptibility to asthma. *Ann NY Acad Sci* 923:303–306, 2000
17. Zhang Z, Kundu GC, Yuan CJ, *et al*: Severe fibronectin-deposit renal glomerular disease in mice lacking uteroglobin. *Science* 276: 1408–1412, 1997
18. Greene T, Lau J, Levey A: Interpretation of clinical studies of renal disease (chapt 40), in *Immunologic Renal Diseases*, edited by Couser W, Philadelphia, Lippincott-Raven, 1997, pp 887–911
19. Martin ER, Lai EH, Gilbert JR, *et al*: SNPing away at complex diseases: Analysis of single-nucleotide polymorphisms around APOE in Alzheimer disease. *Am J Hum Genet* 67:383–394, 2000
20. Pilon AL: Rationale for the development of recombinant human CC10 as a therapeutic for inflammatory and fibrotic disease. *Ann NY Acad Sci* 923:280–299, 2000
21. Galla JH: Molecular genetics in IgA nephropathy. *Nephron* 88: 107–112, 2001

Kidney International, Vol. 61 (2002), pp. 2044–2057

Fractalkine expression and the recruitment of CX_3CR1^+ cells in the prolonged mesangial proliferative glomerulonephritis

YUMI ITO, HIROSHI KAWACHI, YOSHIO MORIOKA, TAKESHI NAKATSUE, HIROKO KOIKE, YOHEI IKEZUMI, AKIHISA OYANAGI, YASUHIRO NATORI, YUMIKO NATORI, TAKAMICHI NAKAMURA, FUMITAKE GEJYO, and FUJIO SHIMIZU

Department of Cell Biology, Institute of Nephrology, and Division of Clinical Nephrology and Rheumatology, Niigata University Graduate School of Medical and Dental Sciences, Niigata; Division of Pharmacology, Research Institute, International Medical Center of Japan, Tokyo; and Department of Internal Medicine, Kumamoto City General Hospital, Kumamoto, Japan

Fractalkine expression and the recruitment of CX_3CR1^+ cells in the prolonged mesangial proliferative glomerulonephritis.

Background. We established the reversible and the prolonged models of mesangial proliferative glomerulonephritis (GN) with anti-Thy 1 antibody 1-22-3. However, the essential factors leading to the prolonged glomerular alterations have not been identified.

Methods. The expressions of several chemokines and cytokines were compared in the reversible and the prolonged models. Expression of fractalkine and the number of the fractalkine receptor CX_3CR1-positive cells in the glomeruli in the prolonged model were significantly higher than those in the reversible model. Then, the localization of fractalkine and the characteristics of CX_3CR1^+ cells were analyzed in glomeruli. To elucidate the significance of the fractalkine expression, we analyzed the expression in the model treated with angiotensin II receptor antagonist, candesartan.

Results. Immunostaining of fractalkine was detected on endothelial cells on the fifth day, and fractalkine staining also was detected in the mesangial area on day 14. Major parts of the CX_3CR1^+ cells in the glomeruli were macrophages, especially $ED3^+$ cells. Candesartan treatment ameliorated the glomerular morphological findings at six weeks after disease induction. Although the treatment did not ameliorate the morphological finding at two weeks, decreased expression of fractalkine and CX_3CR1^+ were already detected at two weeks in rats treated with candesartan.

Conclusions. Fractalkine expression and the recruitment of CX_3CR1^+ cells in glomeruli might play an important role in the development of the prolonged disease. These expressions could be predictors of the prolonged disease of the mesangial proliferative glomerulonephritis.

Key words: candesartan, $ED3^+$ cell, Thy 1.1 glomerulonephritis, inflammation, cell proliferation, chemokine.

Received for publication April 10, 2001
and in revised form November 27, 2001
Accepted for publication January 24, 2002

© 2002 by the International Society of Nephrology

The acute phase of glomerulonephritis (GN) is characterized by glomerular infiltration of inflammatory cells and the proliferation of mesangial cells [1–8]. It has been proposed that the secretary product from macrophage and lymphocytes plays an important role in the development of mesangial proliferative GN in both human and experimental models [1, 2, 9–12]. Thy 1.1 GN is most commonly used as the model of mesangial proliferative GN [13–16]. However, because the Thy 1.1 model is self-limiting, and glomerular architecture returns to normal within six to eight weeks, it is not available to elucidate the mechanism of the role of the inflammatory cells in the development of the prolonged mesangial alterations. We have previously reported that anti-Thy 1.1 mAb 1-22-3 causes severer mesangial alterations than OX-7 and polyclonal anti-thymocyte serum [17]. A single injection of mAb 1-22-3 to uninephrectomized rats caused the prolonged mesangial alterations (prolonged model), although the mesangial alterations induced by an injection of mAb 1-22-3 into rats without uninephrectomy were reversible (reversible model) [18]. It is reported that uninephrectomy increased single nephron glomerular filtration rate (GFR) in the remaining kidney, and also promoted several cytokines production [19]. These alterations caused by uninephrectomy are considered to affect the outcome of the disease, although the precise mechanisms of mesangial alterations in the prolonged model have not been fully elucidated to date.

The purpose of this study was to identify the essential factor that causes the prolonged disease. We analyzed the inflammatory responses in glomeruli in the early stage of the prolonged model and the reversible model. We detected that fractalkine expression and the recruitment of fractalkine receptor CX_3CR1-positive cells in glomeruli were significantly higher in the prolonged model than in the reversible model. Fractalkine is a novel

fourth class of chemokine that possesses three amino acid residues between the first and the second cysteines (C-X_3-C motif) [20]. Unlike other chemokines, fractalkine can exist in two forms, either the membrane anchored or soluble form [21]. The soluble C-X_3-C chemokine is reported to have potent chemoattractant activity for T cells and monocytes, and the membrane-anchored fractalkine, which is mainly expressed by endothelial cells, promotes strong adhesion of those leukocytes. Feng et al recently reported that fractalkine has an essential role in the crescent formation of anti-glomerular basement membrane (GBM) GN in WKY rats [22, 23]. They suggested that fractalkine may be especially important for leukocyte recruitment in tissues with a high blood flow rate, for example, in glomeruli, where the low-affinity binding of other chemokines to proteoglycan may not withstand the high shear environment [22]. These characteristics of fractalkine taken together with our findings, we hypothesized that fractalkine plays an important role in the recruitment and adhesion of inflammatory cells in glomeruli of nephrectomized rats injected with mAb 1-22-3, the glomerular filtration of which was increased.

To elucidate the significance of the fractalkine expression for the development of the disease, we analyzed the expression in the model treated with angiotensin II type I receptor antagonist (AT1RA), candesartan. We observed that the decreased expression of fractalkine and CX_3CR1^+ at two weeks in rats treated with AT1RA, although the treatment did not ameliorate the morphological finding at two weeks. We confirmed that AT1RA treatment ameliorated the glomerular morphological findings at six weeks after disease induction, suggesting that these expressions could be predictors of a prolonged disease in course of mesangial proliferative glomerulonephritis. This study further examined the localization of fractalkine expressing cell and determined the subpopulation of leukocyte CX_3CR1^+ cells. Immunofluorescence (IF) studies suggested that fractalkine was expressed by endothelial cells in the early phase and also by mesangial cells in the late phase. Almost all CX_3CR1^+ cells in glomeruli attracted by fractalkine were not T cells but macrophages. The major parts of CX_3CR1^+ cells in glomeruli were the $ED3^+$ cells that are reported to be activated macrophages. These results suggest that fractalkine and CX_3CR1^+ cells attracted by fractalkine are involved in the development of prolonged mesangial proliferative GN.

METHODS

Animals

Specific pathogen free female Wistar rats (6 weeks old) were purchased from Charles River Japan Inc. (Atsugi, Japan).

Induction of the uninephrectomized prolonged model

Sixty rats were divided into two groups: (*a*) thirty rats were uninephrectomized two weeks before injection of 1.0 mL of saline containing 0.5 mg monoclonal antibody (mAb) 1-22-3; (*b*) thirty rats were sham operated two weeks before the injection of 1.0 mL of saline containing 0.5 mg mAb 1-22-3. Five rats in each group were sacrificed at 30 minutes, 24 hours, and 5, 14, and 56 days after the injection of mAb 1-22-3. Five rats of each group were sacrificed before the injection of mAb 1-22-3 as a control of the baseline (0 hour). As controls, five rats were injected with phosphate-buffered saline (PBS) two weeks after the unilateral nephrectomy, and sacrificed on 56 days after the injection. Unilateral nephrectomy and sham operations were performed under ether anesthesia. A small flank incision was made, the left renal capsule and the adrenal gland were separated from the kidney, the renal artery, vein, and ureter were ligated at renal pedicle and the left kidney was removed. The sham operation involved the same surgical procedure, but the kidney and the renal pedicle were undamaged.

Urinary protein excretion

Urine was collected from the rats in a metabolic cage for 24 hours, and 1, 7, and 14 days after the surgery, and 1, 3, 5, 7, 14, 21, 28, 35, 42, 48, and 56 days after the mAb 1-22-3 or PBS injection. The amount of urinary protein excretion was measured by the Bradford method (Bio-Rad, Oakland, CA, USA).

Morphological and immunohistochemical studies

The right kidney of each rat was removed immediately. For light microscopy, part of the kidney was fixed with Carnoy's solution, embedded in paraffin and a section was stained with periodic acid-Schiff (PAS) and periodic acid-methenamine silver (PAM). Mesangial matrix expansion was analyzed semiquantitatively as grades from 0 to 4 according to the method of Raij, Azar and Keane [24]. The severity of mesangiolysis at 24 hours after the mAb 1-22-3 injection was scored by 0 to 4 according to the method described by Johnson et al [25].

For immunofluorescence microscopy, renal tissue was quickly frozen in n-hexane and cooled to −70°C. Four-micrometer thick sections were cut by cryostat. These sections were incubated with anti-α-smooth muscle actin (α-SMA) antibody, (Sigma St. Louis, MO, USA) or anti-rat collagen type I antibody (Chemicon, Temecula, CA, USA), and then stained with FITC-conjugated anti-mouse IgG2a or FITC-conjugated anti-rabbit IgG (Southern Biotechnology Associates, Birmingham, AL, USA), respectively. The intensity of α-SMA and collagen type I staining was scored as the method described by Floege et al [26]. To identify the subpopulation of inflammatory cells recruited in glomeruli, the cryostat sections were

incubated with anti-leukocyte common antigen (OX-1; Serotec, Oxford, UK), anti-PMN (RP-3; kindly donated by Dr. Sendo, Yamagata University, Japan), anti-pan macrophage (ED1; Chemicon), anti-activated macrophage (ED3; Chemicon), anti-pan T cell (OX-19; European Collection of Animal Cells, Porton Down, Salisbury, UK), and then stained with FITC-conjugated anti-mouse IgG1 (Southern Biotechnology Associates) for OX-1, ED1, and OX-19, or FITC conjugated anti-mouse IgG2a for ED3, or FITC conjugated anti-mouse IgM (Southern Biotechnology Associates) for RP-3. The number of positive cells for these markers was counted in 30 full sized glomeruli. The numbers were expressed as the mean cells per glomeruli.

Immunostaining of fractalkine

Rabbit anti-rat fractalkine antibody was purchased from Torrey Pines Biolabs, Inc. (San Diego, CA, USA). To confirm the specificity of the staining of the anti-fractalkine antibody, the antibody was absorbed with the fusion protein of the chemotactic site of the fractalkine of rat. Chemotactic site of rat fractalkine coding 76 amino acid residues and engineered with EcoRI (5′) and SalI (3′) restriction sites so as to maintain the appropriate reading frame were amplified by polymerase chain reaction (PCR), and directly subcloned with pGEX-6P-1 vector (Amersham Pharmacom Biotech, Buckinghamshire, UK). Following bacterial transformation, cells of bacterial culture were pelleted, washed, solubilized, and applied in sodium dodecyl sulfate-polyacrylamide gel electrophoresis (SDS-PAGE). Fusion protein was extracted from acrylamide gels. As control for absorption test, the fusion protein of pGEX-6P-1 vector without insert was used. The rate of fractalkine positive glomeruli on the 14th day after mAb 1-22-3 injection was determined in randomly selected 20 full sized glomeruli. The glomerulus in which clearly specific staining of fractalkine was detected over 50% area was defined as fractalkine positive glomerulus. To examine the localization of the fractalkine expressing cell, dual labeling IF studies were performed with anti-fractalkine and anti-rat endothelial cell (RECA1; Serotec), or mAb 1-22-3.

Identification of CX_3CR1 expressing cells

To determine which subpopulation of leukocytes the CX_3CR1^+ cells are located, dual-labeling studies were performed. The sections were incubated with anti-CX_3CR1 (Torrey Pines Biolabs, Inc.) and ED1, ED3, or OX-19, and then stained with FITC-conjugated anti-rabbit IgG and TRITC-conjugated anti-mouse IgG (Dako, Glostup, Denmark). The CX_3CR1^+ cells, and double positive cells with ED1, ED3, or OX-19 were counted in 20 full sized glomeruli.

Kidney binding and complement fixation

To compare the amount of mAb 1-22-3 bound to the kidney, each of the three nephrectomized or sham operated rats were injected with mAb 1-22-3 labeled with ^{125}I, and kidneys were removed 30 minutes after the mAb 1-22-3 injection. Monoclonal antibody 1-22-3 was labeled with ^{125}I by the chloramine-T method and the level of ^{125}I bound to the kidneys was measured as described previously [27]. To compare the complement fixation in glomeruli, 30 minutes after the injection the kidney sections were incubated with FITC-conjugated anti-rat C3 (Dako). IF intensity of 30 full sized glomeruli from the sections of five rats of each group was measured by an auto-exposure system (Vanox AHBS3; Olympus, Tokyo, Japan) as described previously [17].

Semiquantitative reverse transcriptase (RT)-PCR

Glomeruli were isolated from kidneys pooled from the same group. The total RNA was extracted from isolated glomeruli by TRIZOL (Gibco BRL, Gaithersburg, MD, USA) and stored at −70°C before use. RNA was quantified by absorbance at 260 nm. First strand cDNA was synthesized by total RNA from each group by using a commercial kit (Superscript preamplification system; Gibco BRL). Five micrograms of RNA was incubated at 42°C for 50 minutes in a final volume of 20 μL, which contained 20 mmol/L Tris-HCl (pH 8.4), 50 mmol/L KCl, 2.5 mmol/L $MgCl_2$, 1 mmol/L each of dATP, dCTP, dGTP and dTTP, 0.5 mg oligo (dT) and 50 U reverse transcriptase (SuperScript II; Gibco BRL). At the end of the incubation, samples were heated at 90°C for five minutes to eliminate the transcriptase activity. Then, 3 μL of cDNA were amplified in a 50 μL total volume of PCR buffer containing 10 mmol/L Tris-HCl (pH 8.3), 50 mmol/L KCl, 1.5 mmol/L $MgCl_2$, 200 mmol/L each dATP, dCTP, dGTP and dTTP, 0.4 mmol/L each of the 5′ and 3′ primers and 2.5 U heat-activated Taq DNA polymerase (AmpliTaq Gold; Perkin-Elmer, Foster, CA, USA). The primers of MCP-1, RANTES, lymphotactin and GAPDH were designed according to published sequence [12, 28]. The primers of fractalkine, CX_3CR1 and macrophage derived chemokine (MDC) were designed based on their sequences. The sequences of the primers, the sizes of PCR product expected and annealing temperature were shown in Table 1. PCR products of fractalkine and CX_3CR1 were sequenced and confirmed to be specific products of rat fractalkine and rat CX_3CR1. Amplification was carried out using the PC-800 programmable temperature control system (Astec, Fukuoka, Japan) through 20 to 35 cycles of denaturation at 95°C for 30 seconds, annealing at individual temperatures for 30 seconds, and extension at 72°C for one minute. The optimum number of amplification cycles used for semiquantitative PCR was chosen based on the pre-

Table 1. Primers used in this study

	Sense primer	Antisense primer	Temperature °C	Size *bp*
MCP-1	5'-CTC TTC CTC CAC TAT GC-3'	5'-CTC TGT CAT ACT GGT CAC TTG-3'	60	457
RANTES	5'-ACC TGC CTC CCC ATA TGG CT-3'	5'-GTA TTC TTG AAC CCA CTT CTT CTT C-3'	60	190
Lymphotactin	5'-CCT GGG AGT CTG CTG CTT CG-3'	5'-TGG CGG ACC TCT GGG CTT GT-3'	60	313
Fractalkine	5'-CTC GCC AAT CCC AGT GAC CTT GCT O-3'	5'-GAT TGG TAG ACA GCA GAA CTC GGC CAA ATG-3'	61	492
TARC	5'-GCG TGC TGC CTG GAT TAC TTC AA-3'	5'-TTC TTC ACA TGT TTG TCT TTG GGG TC-3'	58	154
MDC	5'-TGG CAC TTC AGA CCT CCG ATG-3'	5'-AGG GGA CGG ACA GGA AGT ACA-3'	58	398
CX_3CR1	5'-AGC TGC TCA GGA CCT CAC CAT-3'	5'-GTT GTG GAG GCC CTC ATG GCT GAT-3'	61	319
GAPDH	5'-CTC TAG CCA CGG CAA GTT CAA-3'	5'-GGA TGA CCT TGC CCA CAG C-3'	60	516

liminary trial in the linear phase of amplification. The PCR products were electrophoresed on 1.2% agarose gel containing 0.0001% ethidium bromide in TAE buffer, and band intensities were determined by image analysis using a Macintosh computer and the densitometry program, Densitograph (ATTO, Tokyo, Japan). All results were corrected for the amount of mRNA of GAPDH as an internal standard. The data are shown as ratios relative to control rat expression (0 hr of the sham operated group) and are expressed as mean ± SD of these independent experiments.

Real-time RT-PCR

Real-time PCR was performed basically according to the manufacturer's manual. cDNA was synthesized as described above. cDNA, specific primers and SYBR Green (Takara, Otsu, Japan) were mixed with *Takara Ex Taq* R-PCR Version For Real Time PCR kit (Takara). PCR reactions were run on Smart Cycler System (Takara). The sequences of the primers of fractalkine and GAPDH were described above. The reactions and run for all samples were performed in duplicate.

Preparation and chemotaxis analysis of inflammatory leukocytes from nephritic glomeruli

Inflammatory leukocytes were isolated from glomeruli of rats sacrificed on day 5 after 0.5 mg of mAb 1-22-3 injection following the method of Cook, Smith and Cattell [29]. Glomerular leukocytes were resuspended at 1×10^6/mL in MEM plus 10% heat-inactivated fetal calf serum (FCS). Chemotaxis analysis was performed basically according to the method described by Chen et al [23]. In brief, 200 μL of 10^{-7} mol/L human recombinant fractalkine (Genzyme/Techne, Cambridge, MA, USA) diluted with PBS with 1 mg/mL BSA was placed in the lower well of the blind well chamber, model BW 200S (Neuro Probe, Inc., Cabin John, MD, USA), and separated from 200 μL of cell suspension by an 5-μm pore size polyvinylpyrolidone-free polycarbonate filter (Neuro Probe, Inc). After incubation at 37°C for two hours, sedimented cells on the top surface of the filter were wiped off and migrated cells on the undersurface were fixed in methanol for 30 seconds, and stained with Giemsa's solution (Merck Japan, Tokyo, Japan). The cell numbers were counted with four filters. Results were expressed as mean ± SEM cell number per low power fields (×200). As control, PBS with 1 mg/mL BSA was placed in the lower chamber. For the immunofluorescence (IF) study, the migrated cells on the undersurface of the filters were stained with ED3 and FITC anti-mouse IgG2a, after the sedimented cells on the top surface of the filter were wiped off.

Effect of AT1RA on the expression of fractalkine and CX_3CR1

To analyze the long-term consequence of AT1RA, candesartan treatment, the prolonged mesangial GN was induced by a single injection of 0.5 mg mAb 1-22-3 into uninephrectomized rats. Six rats of each group were injected daily from day 0 (1 hour after disease induction) through experimental period intraperitoneally with 0.5 mg/kg body wt/day of candesartan or PBS basically according to the method described previously [30] and then sacrificed at six weeks after disease induction. Mesangial matrix expansion was scored as described previously. To analyze the effect of AT1RA candesartan on the expressions of fractalkine and CX_3CR1, the prolonged mesangial GN was induced in 12 rats as described above. Six rats of each group were injected daily with candesartan or PBS as described above, and then sacrificed on day 14 after disease induction. The expression of fractalkine and the recruitment of CX_3CR1^+ cells were counted in 30 full sized glomeruli. For further analyses of mRNA expressions of chemokines and renal function, the prolonged mesangial GN was induced in 10 rats. Five rats each were injected with candesartan, or PBS and then sacrificed on day 14 after disease induction. Glomerular RNA was prepared from pooled kidney of each group. mRNA expressions for fractalkine, CX_3CR1, MCP-1 and MDC were analyzed by semiquantitative RT-PCR. Glo-

Table 2. Kidney bound mAb1-22-3, complement fixation, and mesangiolysis score

Group	Kidney bound mAb1-22-3 *μg/kidney* ($N = 3$)	C3 fluorescence intensity *seconds* ($N = 5$)	Mesangiolysis score ($N = 5$)
Uninephrectomized	11.29 ± 1.63	15.46 ± 3.51	2.75 ± 0.96
Sham operated	8.55 ± 1.87	12.4 ± 3.40	2 ± 0

The C3 fluorescence intensity in glomeruli was expressed as the autoexposure time that was considered to reciprocally reflect the staining intensity.

merular mRNA expression of fractalkine was also analyzed by the real-time RT-PCR method. Systolic blood pressure (SBP) was measured in conscious, restrained rats using a tail-cuff sphyngmanometer on day 11 after disease induction. Serum levels of creatinine were measured on day 14 according to the standard method. Creatinine clearance (C_{Cr}) was calculated from a urine sample taken 24 hours before the animal was sacrificed.

Expression of fractalkine and CX_3CR1 in the prolonged model induced by two consecutive injections of 1-22-3

To investigate the expression in another prolonged model, the prolonged mesangial alterations were induced by two consecutive injections of 1.0 mL of saline containing 0.5 mg of mAb 1-22-3 twice an interval of two weeks as already reported [31]. As control, the reversible mesangial alteration was induced by injecting once with 0.5 mg of the mAb 1-22-3. The rats of each group were sacrificed 30 minutes, 24 hours, 5, and 14 days after the last injection. Glomerular mRNA expressions of fractalkine and CX_3CR1 were examined by RT-PCR.

Statistical analysis

Statistical significance was evaluated using the unpaired t test or the Mann-Whitney U test. All values were expressed as the mean ± SD. Differences at $P < 0.05$ were considered significant. Data were analyzed using StatView for Macintosh (Abacus Concepts, Berkeley, CA, USA).

RESULTS

Initiation events, urinary protein excretion and the mesangial alterations of the uninephrectomized prolonged model

The amount of kidney binding mAb 1-22-3, C3 fluorescent intensity and the mesangiolysis score of uninephrectomized and sham operated groups were summarized in Table 2. There was no statistically significant difference in the intensity of the C3 deposition and the mesangiolysis score in both groups. The kinetics of urinary protein excretion was shown in Figure 1A. The amount of urinary protein excretion peaked on day 3 after injection in both groups. No difference of the amount of proteinuria on days 5 and 7 was detected between both groups. Although urinary protein excretion of the sham operated group decreased gradually and normalized by four weeks after the injection, abnormal proteinuria persisted for two months in the uninephrectomized group. No abnormal proteinuria was detected

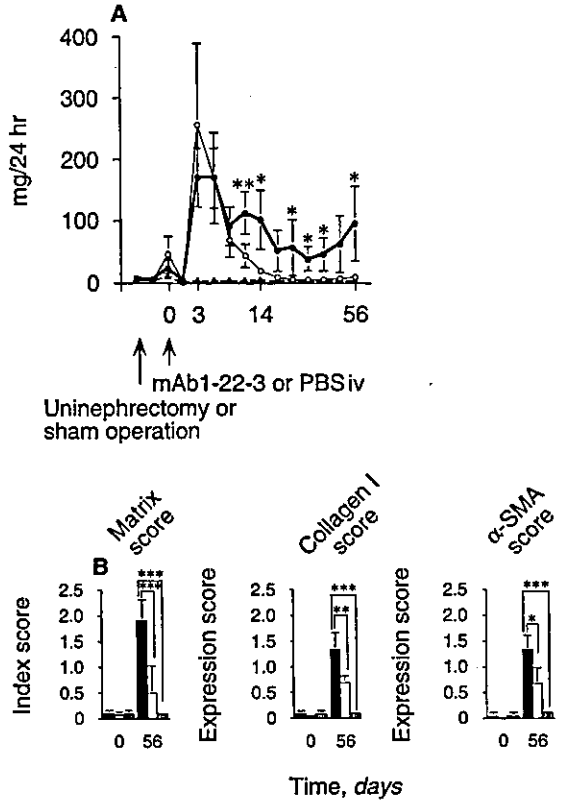

Fig. 1. (A) Time course of urinary protein excretion after monoclonal antibody (mAb) 1-22-3 injection. The amount of 24-hour proteinuria was measured 1, 7 and 14 days after the surgery and 1, 3, 5, 7, 14, 21, 28, 35, 42, 48, and 56 days after the mAb 1-22-3 or PBS injection. Symbols are: (●) uninephrectomy + 1-22-3; (○) sham operation + 1-22-3; (▲) uninephrectomy + PBS. Abnormal proteinuria persisted for 2 months in the uninephrectomized group, whereas urinary protein excretion in the sham operated group was normalized by the 28th day after mAb 1-22-3 injection. No abnormal proteinuria was detected in uninephrectomized rats without injection of mAb 1-22-3. (*B*) Matrix score, collagen type I score, and α-SMA score in the uninephrectomized and sham operated groups. Symbols are: (■) uninephrectomy + 1-22-3; (□) sham operation + 1-22-3; (▩) uninephrectomy + PBS; $^*P < 0.05$; $^{**}P < 0.01$; $^{***}P < 0.005$. The mesangial matrix expansion and the extension of αSMA and collagen type I staining on the 56th day was higher in the uninephrectomized group than in the sham operated group.